

AUTOMATIC CLASSIFICATION OF MEDICAL X-RAY IMAGES

Mohammad Reza Zare¹, Woo Chaw Seng², Ahmed Mueen³

^{1,2}Department of Artificial Intelligence,

Faculty of Computer Science and Information Technology,

University of Malaya, Malaysia

³Faculty of Information Technology,

King Abdulaziz University, Saudi Arabia

Email: mreza_zare57@yahoo.com, cswoo@um.edu.my, mueen123@gmail.com

ABSTRACT

Image representation is one of the major aspects of automatic classification algorithms. In this paper, different feature extraction techniques have been utilized to represent medical X-ray images. They are categorized into two groups; (i) low-level image representation such as Gray Level Co-occurrence Matrix(GLCM), Canny Edge Operator, Local Binary Pattern(LBP), pixel value, and (ii) local patch-based image representation such as Bag of Words (BoW). These features have been exploited in different algorithms for automatic classification of medical X-ray images. We then analyzed the classification performance obtained with regard to the image representation techniques used. These experiments were evaluated on ImageCLEF 2007 database consists of 11000 medical X-ray images with 116 classes. Experimental results showed the classification performance obtained by exploiting LBP and BoW outperformed the other algorithms with respect to the image representation techniques used.

Keywords: Classification, X-Ray, Image Processing

1.0 INTRODUCTION

We are living in the age of multimedia information technologies burdened by information overdose. A wide availability of digital devices such as digital cameras, scanners, mobile phones, notebooks at reasonable prices accelerate the growth of multimedia content production. There is also an increase of digital information in medical domain where medical images of different modalities i.e., X-rays, CT scans, MRI scans, etc., are produced everyday in massive numbers. For instance, over 640 million medical images were stored in more than 100 National Health Service Trust in UK, as of March 2008 [1]. Medical image databases are the key component in diagnosis and preventive medicine. While medical image databases show a wealth of information, it also creates a problem in terms of retrieving the images. As a result, there is an increased demand for a computerized system to manage these valuable resources. In addition, managing such data demands high accuracy since it deals with human life.

Due to the immense need of effective and accurate medical image retrieval application, new trends for image retrieval using automatic image classification has been investigated for the past few years. It is believed that the quality of such medical system can be improved by a successful classification of images so that the irrelevant images can be filtered out.

Automatic image classification is mapping images into pre-defined classes and it involves some basic principles such as representation where visual feature of the image are extracted and generalization which is training and evaluating the classifier. The first and most vital component of any classification system is image representation. It is categorized into two main approaches, (i) low-level image representation and (ii) patch based image representation. Low-level image representation has been used by several researchers in various domains [2-9][28]. Seong-Hoon *et al.* [2] proposed classification of medical x-ray images where texture information of medical x-ray images are extracted using LBP; the classification accuracy obtained outperforms others who use edge histogram descriptor. Combination of block based local binary pattern with edge histogram was used as medical image representation for the task of automatic medical image annotation in ImageCLEF 2007 [3]. Zhy *et al.* [4] applied

segmentation method on ultrasound medical images based on texture features which are obtained according to GLCM. GLCM were combined with histogram moments as feature extraction to classify ultrasound medical images in [5]. Another widely used strategy is combining different local and global descriptors into a unique feature representation. Pixel value as global image descriptor was combined with other image representation techniques to construct feature vector of the image [6-9].

Recently, more promising studies have been focused on local patch based image representation. The bag of words (BoW) represents images using histograms of quantized appearances of local patches. In recent years, many studies exploited this feature in various image classification domains including medical domain [10-20]. With increasing size of medical X-ray archives, it is important to have simplistic, discrete representations and simple matching measures to preserve computational efficiency. It is argued that BoW paradigm provides efficient means to address the challenge of CBIR system in large size databases such as the one in ImageCLEF [10]. They proposed X-ray image categorization and retrieval based on local patch representations using a “bag of visual words” approach. They analyzed the effects of various parameters on system performance. The best result was presented using dense sampling of simple features and a nonlinear kernel-based Support Vector Machine (SVM). This was an extension of another work where visual words dictionary were generated to represent X-Ray chest Images [11]. Deselaers *et al.* in [12] extracted features from local patches of different sizes which were taken at every position and were scaled down to a common size. In that work, rather than using a dictionary, the feature space was quantized uniformly in every dimension and the image was represented as a sparse histogram in the quantized space.

In this paper, both of the above categories of image representation techniques are incorporated in different experiments for the task of automatic classification of medical X-ray images. The rest of the paper is organized as follow. Section 2 presents the proposed approach in detail. Experimental results and discussion are reported and analyzed in section 3 and section 4 respectively. Finally, the overall conclusions of this study are presented in section 5.

2.0 METHODOLOGY

The classification process consists of two steps, i.e. training phase and testing phase. In the training phase, the selected features are extracted from all the training images, and the classifier is trained on the extracted features to create a classification model. This model is then used to classify the test images into the predefined categories in the testing phase. Fig. 1 illustrates the training phase of the proposed classification framework.

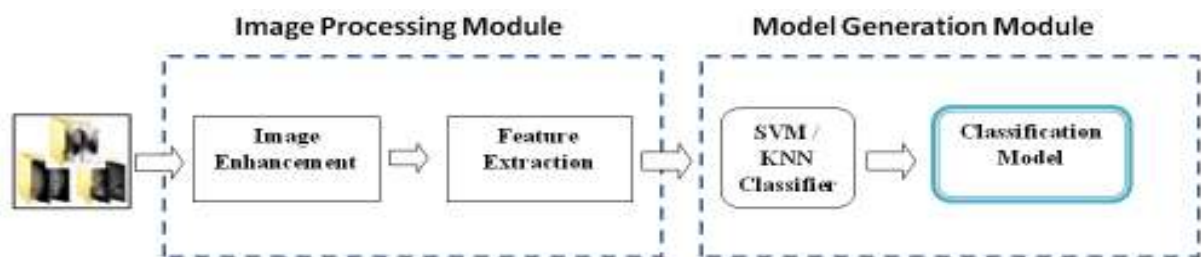


Fig. 1: General Classification Framework (Training Phase)

2.1. Image Processing Module

Training phase consist of two modules; Image Processing and Model Generation. The image processing module composed of image enhancement and feature extraction as shown in Fig. 1.

2.1.1. Image Enhancement

Histogram equalization as one of the image enhancement techniques is applied to improve the quality of the image such as increasing the contrast of the image. This contrast adjustment provides better gray intensities distribution on

the histogram. The method is useful in images with backgrounds and foregrounds that are both bright or both dark. In particular, the method can lead to better views of bone structure in X-ray images [8].

2.1.2. Feature Extraction

The second component of image processing module is feature extraction. It plays an important role in the performance of any image classification because it can produce significant impact on the results of classification. Numerous low-level features such as color, texture shape are described in existing literature review. However, as X-ray images are gray level images and do not contain any color information, the related CBIR systems mostly deal with textures and shape for feature extraction process. Different approaches for feature extraction have been employed in this experiment as explained below.

2.1.2.1. Texture

Texture contains important information regarding underlying structural arrangement of the surfaces in an image. Gray Level Co-occurrence Matrices (GLCM) [21] and Local Binary Patterns (LBP) introduced by Ojala et al. [22], the commonly used feature extraction techniques, are employed as for texture features.

GLCM is one of the well-known texture extraction techniques which measures second order texture characteristics. The GLCM of an $N \times N$ image, containing pixels with gray levels $0, 1, 2, \dots, G-1$ is a matrix $C(i, j)$, where each element of the matrix represents the probability of joint occurrence of intensity levels i and j at a certain distance and an angle θ . In this thesis, the four occurrence matrixes of GLCM are obtained from four different directions ($\theta \in \{0^\circ, 90^\circ, 45^\circ, \text{ and } 135^\circ\}$) at global level.

Another important texture feature used in this thesis is LBP. Original LBP describes only global texture information. On the other hand, local features are more robust to occlusion and clutter. Therefore, the image was divided into 4×4 non-overlapping sub-images and then each sub-image was further divided into non-overlapping square image block as the same size of 'neighbor set'. The local LBP distribution for each square block included in sub-image can be represented as a histogram having 59 bins and final histogram of each sub-image was generated by combining local histograms. Since there are 16 sub-images, a total of $59 \times 16 = 944$ histogram bins are generated for feature vector.

2.1.2.2. Shape

Shape provides geometrical information of an object in an image. This geometrical information is remained same even when the location, scale and orientation of the object are changed. In this study, the shape information of an image is described based on its edges. A histogram of the edge directions is used to represent shape attribute for each image and image patches. Canny edge operator [23] is used to generate edge histograms. The algorithm of Canny edge detector is run in 5 different stages as follow:

- Smoothing: To remove noise by using Gaussian filter.
- Finding gradients: Finding the intensity gradient of the image, by using finite-difference approximations for the partial derivatives to calculate gradient magnitude and orientation.
- Non-maximum suppression: Only local maxima should be marked as edges. This will be obtained by applying non-maxima suppression to the gradient magnitude.
- Double thresholding: Potential edges are determined by thresholding.
- Edge tracking by hysteresis: Final edges are determined by suppressing all edges that are not connected to a very certain (strong) edge.

2.1.2.3. Pixel Value

Pixel value is the simplest form of image representation technique. In this approach, the images are scaled down to common size and represented by a feature vector that contains image pixel values. It is argued that image pixel value does not provide good classification or retrieval results as it is difficult to find which two pixels should be evaluated when comparing two images. However, it has been shown that this method serves as a reasonable baseline for classification and retrieval of simple images with few objects such as medical X-ray images and character recognition [24].

2.1.2.4. Bag of Words

The process of BoW started with detecting local interest point. Local interest point detectors have the task of extracting specific points and areas from images which are invariant to some geometric and photometric transformations. One of the popular approaches for the detection of local interest point is Difference of Gaussians (DoG) which is used in this experiment. DoG detector proposed by Lowe [25] has been built to be invariant to translation, scale, rotation, and illumination changes and samples images at different locations and scales.

Next, distinctive feature that characterizes a set of keypoints for an image is extracted. Scale Invariant Feature Transform (SIFT) proposed by Lowe [26] is used to describe the grayscale image region around each keypoint in a scale and orientation invariant fashion. Each detected region is represented with the SIFT descriptor with the most common parameter configuration: 8 orientations and 4×4 blocks, resulting in a descriptor of 128 dimensions.

Next step in implementation of bag of visual words is the codebook construction where the 128-dimensional local image features have to be quantized into discrete visual words. This task is performed using clustering or vector quantization algorithm. This step usually uses k-means clustering method, and use cluster center as visual vocabulary term. Upon identification of cluster centers, each image is represented as histograms of these cluster centers by simply counting the frequency of the words appear in an image. To accomplish this task, each feature vector in an image is assigned to a cluster center using nearest neighbor with a Euclidean metric.

2.2. Model Generation Module

As illustrated in Fig. 1, the next module after image processing is model generation. Note that the training set as well as the label of every images have been identified. Upon extraction of visual features from the entire training set, the extracted features as well as the label of every image in the dataset are fed into classifier to construct the classification model. Based on empirical results and several classification applications in same domain, Support Vector Machine (SVM) and K-Nearest Neighbor (KNN) have shown a better classification performance as compared with other classification techniques.

SVM is very attractive for image classification as its aim to find the best hyperplane separating relevant and irrelevant vectors maximizing the size of margin. This optimum hyperplane has the maximum margin towards the sample objects, that is, the greater the margin, the less the possibility that any feature vector will be misclassified.

KNN is the most straightforward and simplest classifier in machine learning techniques. The KNN classification is based on majority vote of k-nearest neighbor classes. Classification is achieved by identifying the nearest neighbours to query example and using those neighbors to determine the class of query. In this work, $k=9$ is used, that means that the algorithm will take majority vote of its 9 nearest neighbors.

3.0 EXPERIMENTAL RESULTS

In this section, set of experiments were conducted to evaluate the classification performance obtained with respect to various image representation techniques. The database used in this research was ImageCLEF 2007 [27]; this dataset contains 11,000 X-Ray images from 116 categories which differ from each other either on account of image modality, examined region, body orientation and biological system examined. 20% of 11,000 training images were

taken as test images to ensure that each class has representation in testing data and the remaining 80% are taken as training images.

3.1. Experiment 1

Fig. 2 represents the process of the first experiment. The following steps are involved in this experiment:

- Texture Features (co-occurrence matrix) are extracted from each image.
- Shape features are extracted from each image.
- The original image is resized to 15×15 pixel resolution to get the pixel vector.
- All the above extracted features are combined into one vector. The total dimensionality of the feature vector for this experiment reached to 278.
- SVM with RBF and KNN with K value 9 are used for classification.

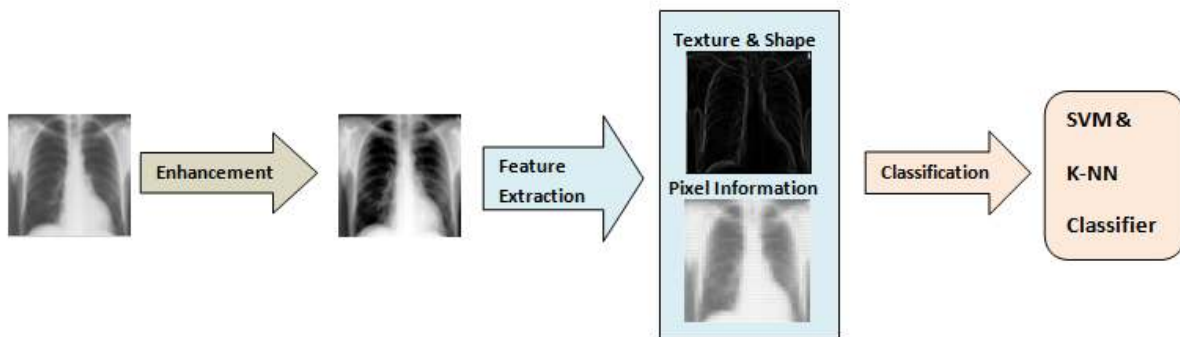


Fig. 2: Block Diagram of the First Experiment

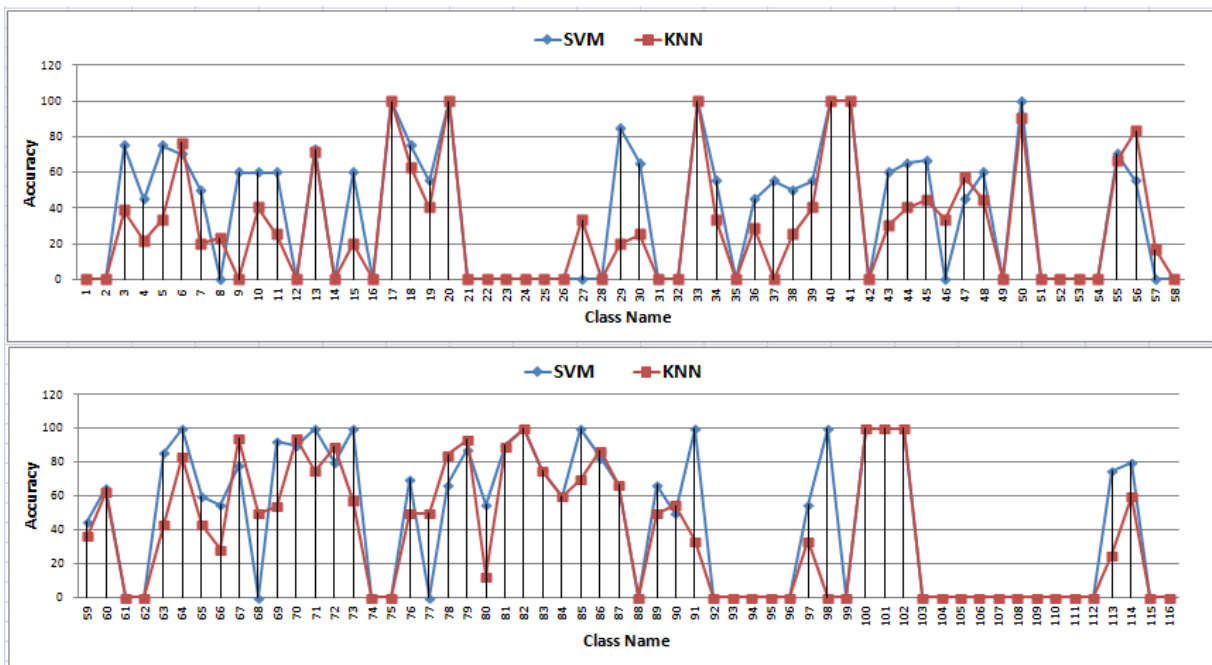


Fig. 3: Classification Result for First Experiment using SVM & KNN

The Fig. 3 depicts the classification accuracy of the first experiment with two different classifiers; SVM and K-NN. The total classification accuracy obtained with SVM and KNN is 70.45% and 65.95% respectively. The result from Fig. 3 demonstrate that from 116 classes, the accuracy rate of 16 classes were 100% using SVM, and 9 classes obtained 100% accuracy using KNN. It also represent that 22 and 18 classes attained the recognition rate of more than 60% with SVM and KNN, respectively. From the figure, it can be seen that 47 classes have classification accuracy of 0 %. This is because that all these classes have less than 15 training images and this would affect on their classification result as well as intra-class and inter-class similarity in images.

3.2. Experiment 2

The process of the second experiment is shown in Fig. 4. The steps involved in this experiment are as below:

- Each image is divided into 4×4 non-overlapping sub-images
- Local binary pattern are extracted from each sub region and combined with each other at the end. Since there are 16 sub-images, a total of 59×16=944 histogram bins are generated for feature vector
- SVM with RBF and KNN with K value 9 are used for classification. The classification result is represented in Fig. 5.



Fig. 4: Block Diagram of the Second Experiment

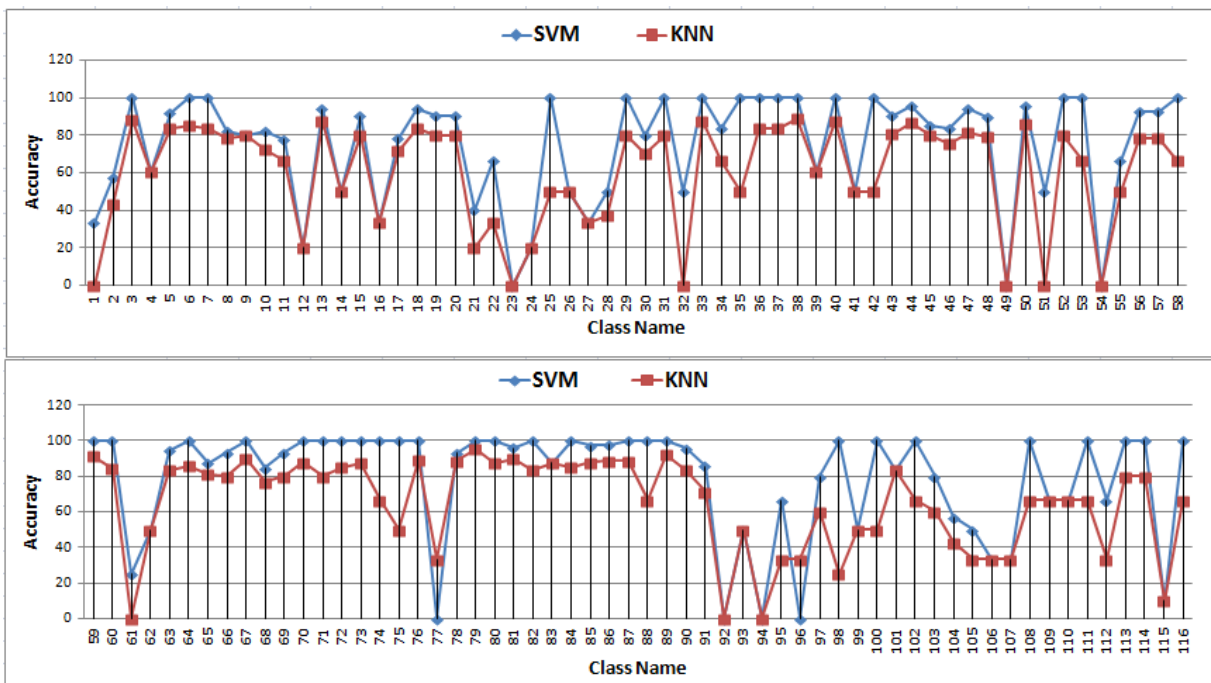


Fig 5: Classification Result for Second Experiment using SVM & KNN

Fig. 5 shows the result of image classification using local binary pattern with SVM and KNN classifiers. Total accuracy rate of 90.7% with SVM and 86 % with KNN obtained. As it can be seen in Fig. 5, there is significant increase in classification accuracy compare with previous experiment. In spite of small number of training images, classes like 2, 3, 9, 14, 29, 31, 37, 51, 52, 88, 96, etc. attain accuracy rate of 100% with both SVM and KNN classifier while it was only zero in previous experiment.

3.3. Experiment 3

The process of third experiment is illustrated in Fig. 6 and the following steps are involved in this experiment:

- Texture Features (co-occurrence matrix) are extracted from each image.
- Shape features are extracted from each image.
- The original image is resized to 15×15 pixel resolution to get the pixel vector.
- All the above extracted features are combined into one vector G
- Each image is divided into 4 non overlapping sub regions
- LBP are extracted from each sub region and combined with each other at the end into one large vector L
- At the end, vector G and L combined with each other. By adding all, the total feature vector is 750.
- SVM with RBF and KNN with K value 9 are used for classification.

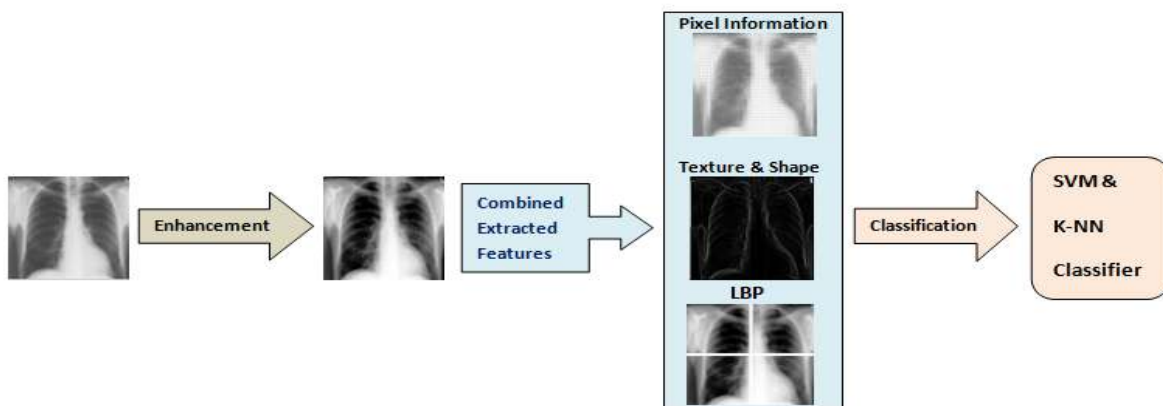


Fig 6: Block Diagram of the Third Experiment

The first two methods were combined to extract the visual features in this experiment and the total classification accuracy is 86.7 % with SVM and 83.2 % with KNN. As shown in Fig. 7, the classification rate is less than the second experiment in despite of increment in selected classes compared with the first two experiments.

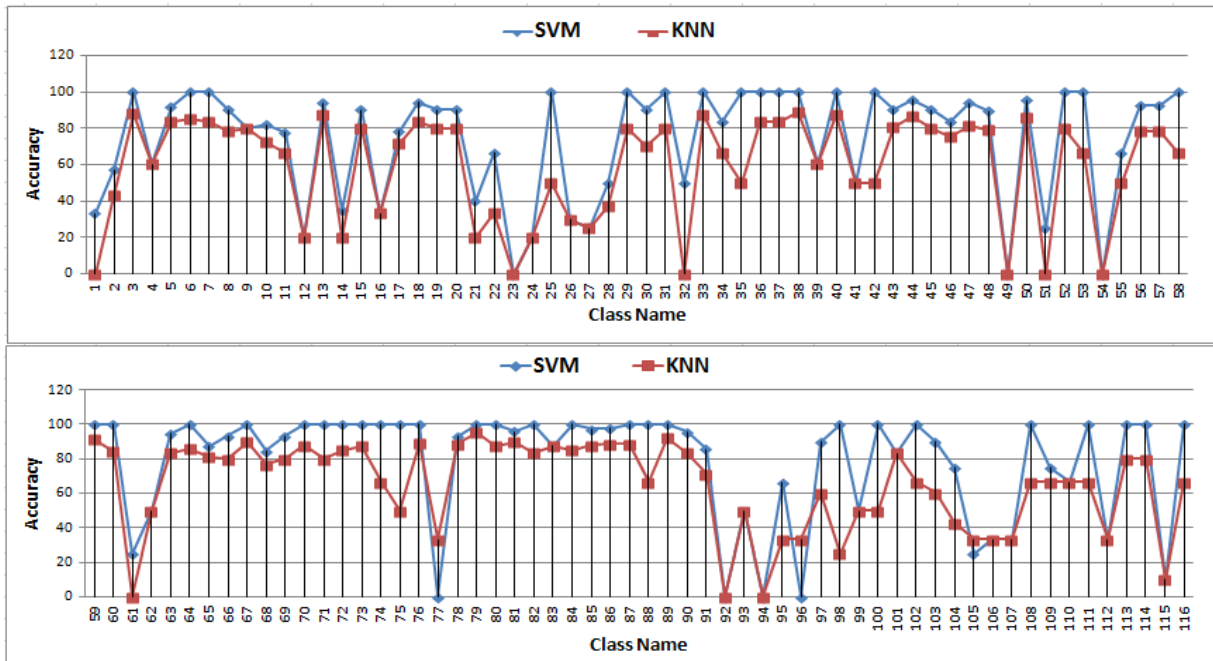


Fig 7: Classification Result for Third Experiment using SVM & KNN

3.4. Experiment 4

In this experiment, BoW are extracted from training images and fed into classifier for constructing the classification model. The total classification rate obtained from the model generated by SVM and KNN classifier are 90% and 86% respectively. Fig. 8 shows the accuracy rate for each individual class obtained by this experiment.

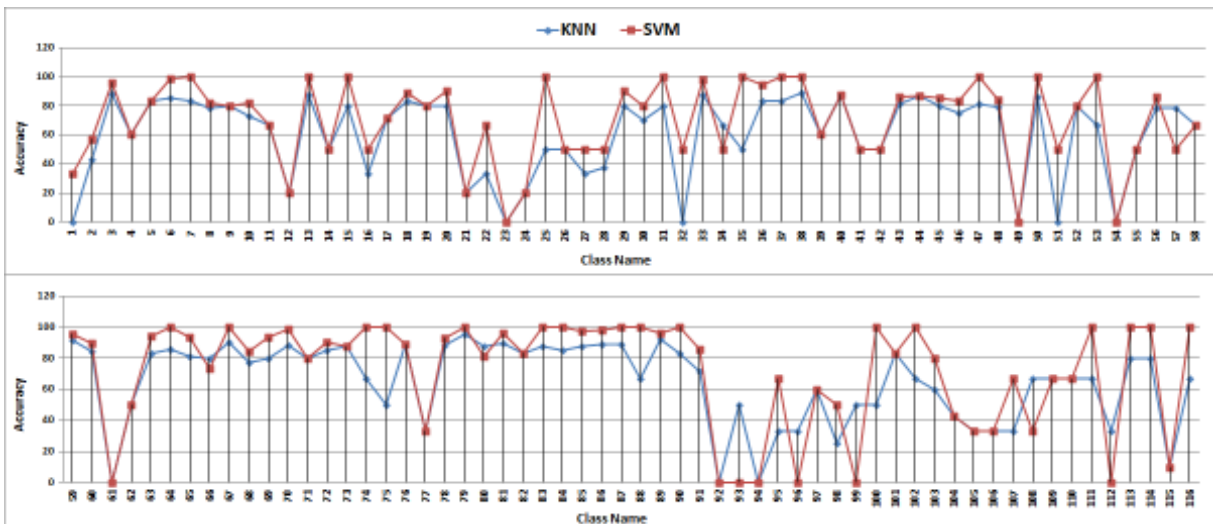


Fig 8: Classification Result for Third Experiment using SVM & KNN

4.0 DISCUSSION

The experimental results showed that the best classification performance obtained are those classification models constructed from LBP and BoW with respect to image representation techniques. However the results obtained are the average accuracy rate. This is not an accuracy rate obtained from every individual class as can be seen from the Figures 3, 5, 7 and 8.

The classification task is difficult due to the unbalanced number of training data as well as the existing high intra-class variability and inter-class similarity among images in some classes. Therefore, it is impossible to obtain high accuracy rate for every individual class in large archive medical database such as ImageCLEF 2007. Intra class variability refers to high visual variability among images even though they belong to the same category. For instance, Fig. 9 shows high intra class variability exists between images in class 27. According to the IRMA code given for this class, these images are labeled as “X-ray, Plain Radiography, Analog, Overview image, coronal, anteroposterior (AP, coronal), upper extremity (arm), hand, carpal bones, musculoskeletal system”.

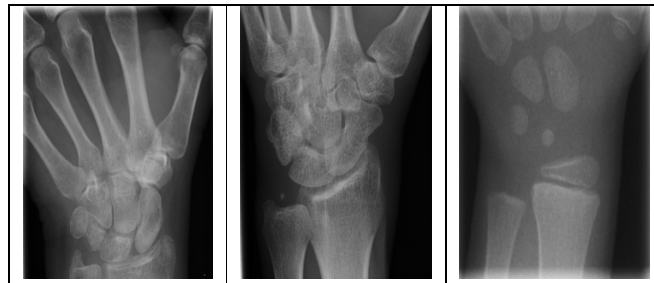


Fig. 9: Intra-class variability within class 27

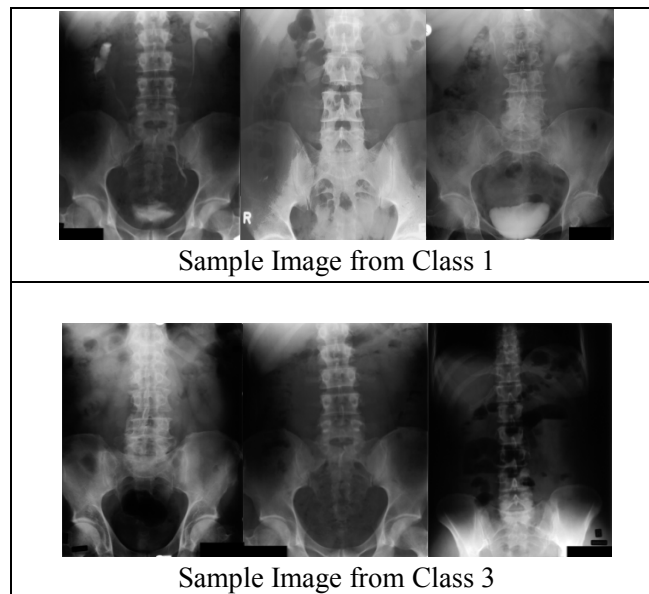


Fig. 10: Inter-class similarity among images from two different classes

Fig. 10 represents an example of inter-class similarity. These images belong to two categories which are differing in term of orientation and biological system even though distinguishing them is a difficult task. Images in upper row belong to class 1 and based on IRMA code annotated as “X-ray, plain radiography, analog, overview image-coronal,



anteroposterior (AP, coronal), supine-abdomenuroipoietic system”, whereas the images in lower row belong to class 3 which are labeled as “X-ray, plain radiography, analog, overview image coronal, posteroanterior (PA), upright-abdomen gastrointestinal system”.

Another difficulty in classification of such medical database is imbalance number of training images among different classes; this is due to the natural commencement of diseases in different part of the body. Therefore it would reflect on probabilities of the routine diagnosis in a radiological clinic. This would result in having a large number of images in selected part of the body while a small number of images in other part of the body.

Table 1 shows sample misclassification results obtained from Experiment 4 which are affected by inter-class similarity and intra class variability. Table 1 contains the following information: the test image and its respective class, the number of training image for that class, two images of output class which the test image is wrongly classified. The test image “Img_ctg_12” belong to class 12 and according to IRMA code given for this class, this image is labeled as “X-ray, plain radiography, analog, overview image, sagittal, unspecified, upper extremity (arm), carpal bones, musculoskeletal system”; but it is misclassified as class 30 which is labeled as “X-ray, plain radiography, analog, overview image, sagittal, unspecified, upper extremity(arm) ,radio carpal joint, musculoskeletal system”. Some sample training images from class 12 are displayed in Fig. 11.

The test image *Img_ctg_99* belongs to class 99 which is misclassified as class 86. There are only 10 training images for class 99 as shown in Fig. 12 while class 86 has 252 training images. According to IRMA code given, images in class 99 are labeled as “X-ray, plain radiography, analog, overview image, coronal, anteroposterior (AP), unspecified, cervical spine, thoraco-lumbar conjunction, musculoskeletal system”; and class 86 is labeled as “X-ray, plain radiography, analog, overview image, coronal, anteroposterior (AP), unspecified, lumbar spine, musculoskeletal system”. As it can be seen from Fig. 11 and Fig. 12, it is obvious that there is intra-class variability within the images in class 12 and class 99 and according to the results shown; the images between these two classes are suffering from intra-class similarity as well. These two mentioned problems as well as lack of training images had led to zero classification accuracy in 31 classes in this experiment.

Table 1: Sample misclassification results obtained from the fourth experiment

Actual Class	No. of Training Image	Test image	Output Class	Sample Image from Output Class
12	23	 Img_ctg_12	30	

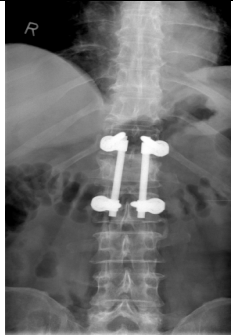
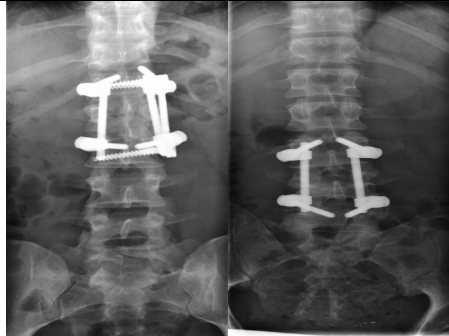
99	10	 <p>Img_ctg_99</p>	86	
----	----	---	----	--



Fig. 11: Sample training images from class 12

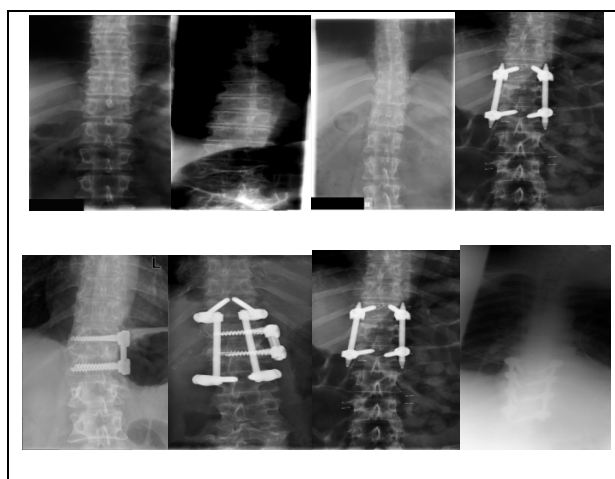


Fig. 12: Sample training images from class 99

5.0 CONCLUSION

The use of image classification is demonstrated to be useful in improving the precision of image retrieval systems. This work presents different methods for automatic X-ray image classification with respect to the image representation techniques used. Image representation is categorized into two groups such as low-level image representation and patch-based image representation. In this paper, GLCM, LBP, Canny Edge Operator and Pixel value are applied as low-level image representation. BoW is used for local patch-based image representation. These features have been employed in different experiments for automatic classification of medical X-ray images. The evaluation for these experiments was conducted on ImageCLEF 2007 medical database. The experimental results indicates those classification methods constructed from LBP and BoW outperformed the other models generated from other representation techniques. However, the measurement used is the average accuracy rate; meaning the classification performance obtained are at global level. This result may not be achievable if we consider every individual class. This shortcoming will be analyzed in our future work. Hierarchical and merged classifiers will be used to rectify this problem.

ACKNOWLEDGMENT

The authors would like to thank Thomas Deserno, Department of Medical Informatics, RWTH Aachen, Germany, for making the database available for the experiments.

REFERENCES

- [1] W. Khaliq et al., "Comparison of a PACS workstation with laser hard copies for detecting scaphoid fractures in the emergency department". *Journal of Digital Imaging*,. Vol. 23, No. 1, 2008, pp.100–103
- [2] K. Seong-Hoon et al., "X-ray image classification using Random Forests with Local Binary Patterns", *International Conference on the Machine Learning and Cybernetics*, 2010
- [3] T. GuangJian et al., "Automatic medical image categorization and annotation using LBP and MPEG-7 edge histograms", *International Conference on Information Technology and Applications in Biomedicine*, 2008
- [4] C. M. Zhy et al., "Segmentation of Ultrasound Image Based on Texture Feature and Graph Cut", *International Conference on the Computer Science and Software Engineering*, 2008
- [5] A. S. M. Sohail et al., "Retrieval and classification of ultrasound images of ovarian cysts combining texture features and histogram moments". *IEEE International Symposium on the Biomedical Imaging: From Nano to Macro*, 2010.
- [6] T. Deselaers et al., "Deformations, patches, and discriminative models for automatic annotation of medical radiographs", *Pattern Recognition Letters*, Vol. 29, No. 15, 2008, pp.2003-2010
- [7] I. Dimitrovski et al., "Hierarchical annotation of medical images", *Pattern Recognition*, Vol. 44, No. 10–11, 2011, pp.2436-49
- [8] A. Mueen et al. , "Automatic Multilevel Medical Image Annotation and retrieval", *Journal of Digital Imaging*, Vol. 21, No. 3, 2008, pp. 290-295
- [9] T. Tommasi et al., "Discriminative cue integration for medical image annotation", *Pattern Recognition Letter*, Vol. 29, No. 15, 2008, pp. 1996-2002
- [10] U. Avni et al., "X-ray Categorization and Retrieval on the Organ and Pathology Level, Using Patch-Based Visual Words", *IEEE Transaction on Medical Imaging* , Vol. 30, No. 3, 2011, pp. 733-746

- [11] U. Avni et al., "Chest x-ray characterization: from organ identification to pathology categorization", *International Conference on Multimedia Information Retrieval*, Philadelphia, 2010
- [12] T. Deselaers et al., "Sparse Patch-Histograms for Object Classification in Cluttered Images", *In: DAGM 2006, Pattern Recognition, 27th DAGM Symposium, Lecture Notes in Computer Science*, Vol. 4174, berlin, Germany, 2006, pp. 201-211
- [13] K. Kesorn et al., "An Enhanced Bag-of-Visual Word Vector Space Model to Represent Visual Content in Athletics Images", *IEEE Transaction on Multimedia*, Vol. 14, No. 1, 2012, pp. 211-222
- [14] W. Zhou et al., "Principal Visual Word Discovery for Automatic License Plate Detection", *IEEE Transaction on Image Processing.*, Vol. 21, No. 9, 2012, pp. 4269-4279
- [15] JM Aman et al., "Content-based image retrieval on CT colonography using rotation and scale invariant features and bag-of-words model", *IEEE International Symposium on Imaging: From Nano to Macro.*, 2010, pp. 1357-1360
- [16] F. Yang et al., "Visual tracking via bag of features", *IET Image Processing*, Vol. 6, No. 2, 2012, pp. 115-128
- [17] L. Sui et al., "Research on pornographic images recognition method based on visual words in a compressed domain", *IET Image Processing*, Vol. 6, No. 1, 2012, pp. 87-93
- [18] S. Lazebnik et al., "Beyond Bags of Features: Spatial Pyramid Matching for Recognizing Natural Scene Categories". *IEEE Conference on Computer Vision and Pattern Recognition*, 2006, pp. 2169-2178
- [19] F. Jie et al., "Bag-of-Visual-Words Based on Clonal Selection Algorithm for SAR Image Classification" , *IEEE Geoscience and Remote Sensing Letters*, Vol. 8, No. 4, 2011, pp. 691-695
- [20] W. Jingyan et al., "Bag-of-Features Based Medical Image Retrieval via Multiple Assignment and Visual Words Weighting", *IEEE Transaction on Medical Imaging*, Vol. 30, No. 11, 2011, pp. 1996-2011
- [21] R.M. Haralick et al., "Textural features for image classification", *IEEE Transaction on System*, Vol. 3, 1973, pp.610-621
- [22] T. Ojala et al., "A Comparative Study of Texture Measures with Classification Based on feature Distributions", *Pattern Recognition*, Vol. 29, 1996, pp.51-59
- [23] J. Canny, "A computational approach to edge detection". *IEEE Trans. Pattern Analysis and Machine Intelligence*, Vol. 8, No. 6, 1986, pp. 679-698
- [24] D. Keysers et al., "Deformation Models for Image Recognition", *IEEE Transaction Pattern Analysis and Machine Intelligence*, Vol. 29, No. 8, 2007, 1422-1435
- [25] D. Lowe , "Object recognition from local scale-invariant features", *International Conference on Computer Vision*, 1999, pp. 1150–1157
- [26] D. Lowe, "Distinctive image features from scale invariant key points", *International Conference on Computer Vision* , Vol. 60, No. 2, 2004, pp. 91-110
- [27] H. Müller et al., "Overview of the ImageCLEFmed 2007 medical retrieval and annotation tasks", *In: Working Notes of the 2007 CLEF Workshop*, 2007

- [28] M.R. Mustaffa et al., "Content-based image retrieval based on color-spatial features", *Malaysian Journal of Computer Science*, 2008, Vol. 21, No. 1, pp. 1-12

BIOGRAPHY

Mohammad Reza Zare received a B.Sc. in Information Technology from Multimedia University in 2005, a M.Sc. in Software Engineering from University of Malaya in 2009. He is currently a PhD candidate at the Department of Artificial Intelligence, University of Malaya.

Dr Woo Chaw Seng is a senior lecturer at the Faculty of Computer Science and Information Technology, University of Malaya. His research interests include image processing and mobile applications.

Dr. Ahmed Mueen is an assistant professor in King Abdul Aziz University Jeddah. He received a B.Sc. in Mathematics from the University Punjab Pakistan in 1993, a M.Sc. in Computer Science from University Putra Malaysia in 1999, and a Ph.D. in Computer Science from University Malaya in 2009. He joined Faculty of Information Technology at Multimedia University Malaysia in 2003, and later he joined King Abdul Aziz University in 2009. Dr. Mueen's research interests include Content-Based Medical Image Retrieval; Information Retrieval; Image Classification; Image Annotation; Medical Image Processing. He has authored 7 refereed journal publications, and more than 10 refereed conference publications.